Journal of Cleaner Production 140 (2017) 1298–1312

Contents lists available at ScienceDirect

Journal of Cleaner Production

journal homepage: www.elsevier.com/locate/jclepro

Review

Insight into catalytic reduction of CO_2: Catalysis and reactor design

Peter Adeniyi Alaba [a, *], Ali Abbas [b], Wan Mohd Wan Daud [a, **]

[a] Department of Chemical Engineering, University of Malaya, 50603 Kuala Lumpur, Malaysia
[b] School of Chemical and Biomolecular Engineering, University of Sydney, NSW 2006, Australia

ARTICLE INFO

Article history:
Received 4 August 2016
Received in revised form
6 October 2016
Accepted 7 October 2016
Available online 8 October 2016

Keywords:
Carbon dioxide
Reduction
Hydrogenation
Reactor
Catalyst
Process intensification

ABSTRACT

Catalytic reduction of CO_2 to produce specialty chemicals or renewable energy sources has attracted immense attention because of the possibility of renewable, sustainable alternative energy, and safer environment. Utilization of CO_2 as an alternative feedstock for synthesis of biorenewable fuel is one of the numerous strategies essential for mitigation of the greenhouse gases emission into the atmosphere. CO_2 reduction occurs at temperature above 413 K and pressure above 1 MPa by using a suitable hydrogenation catalyst. This study investigates the recent advances in catalytic reduction of CO_2 via hydrogenation, focusing on catalysis, reactor, and process intensification. Several factors for the effective catalytic reduction of CO_2 and recent progress in the reactor design for the system are also highlighted.
© 2016 Elsevier Ltd. All rights reserved.

Contents

* Corresponding author.
** Corresponding author.
E-mail addresses: adeniyipee@live.com, ashri@um.edu.my (P.A. Alaba).

http://dx.doi.org/10.1016/j.jclepro.2016.10.022
0959-6526/© 2016 Elsevier Ltd. All rights reserved.

Nomenclature

GHG	Greenhouse gas
IPCC	International Panel on Climate Change
CCS	Carbon dioxide capture and storage
RWGS	Reverse water-gas-shift
GHSV	Gas hourly space velocity
DME	Dimethyl ether
TMC	Transitional metal carbide
PSA	Pressure swing adsorption
CNT	Carbon nanotube
KMC	Kinetics Monte Carlo
ZPE	Zero-point energy
DFT	Density functional theory
CO	Carbon monoxide
CO_2	Carbon dioxide
CH_3OH	Methanol
CuO	Copper oxide
Al_2O_3	Aluminum oxide
$\gamma - Al_2O_3$	Gamma alumina
ZrO_2	Zirconium oxide
ZnO	Zinc oxide
HCO_2^-	Formate
CH_4	Methane
CaO	Calcium oxide
WC	Tungsten carbide
Mo_2C	Molybdenum carbide
SiC	Silicon carbide
TaC	Tantalum carbide
Fe_3C	Iron carbide
MnO	Manganese oxide
Cr_2O_3	Chromium oxide
La_2O_3	Lanthanum oxide
Ga_2O_3	Gallium oxide
MCM-41	Mobil Composition of Matter No. 41
K_2O	Potassium oxide

1. Introduction

Global warming is currently the foremost environmental concern faced by mankind (Valipour, 2012a, 2012b; Yannopoulos et al., 2015). Carbon dioxide, extracted from combustion of fossil fuel, is the chief greenhouse gas (GHG) in the atmosphere that immensely contributes to global climate change (Budzianowski, 2012; McCollum et al., 2014; Roy et al., 2010). CO_2 capture from petrochemical process streams and flares is necessary for reduction of GHG emission into the atmosphere (Alaba, Sani and Daud, 2015b; Ravanchi and Sahebdelfar, 2014; Sani, Alaba, Raji-Yahya, Aziz and Daud, 2016b). The global temperature increase via absorption and re-emission of infrared light is due to the effect of GHG. The GHG effect has global and significant aspects including rising precipitation throughout the earth, ice melting on the Earth pole, and fast increasing sea level (Abnisa and Daud, 2015; Khatib, 2012). International Panel on Climate Change (IPCC) predicted that the level of release of CO_2 to the atmosphere may possibly increase to 590 ppm by 2100 and the average global temperature could increase by ~1.9 °C (Change, 2007). To avoid this, IPCC proposed 50%–85% reduction of global CO_2 emissions relative to 2000 levels by the year 2050 (McGlade and Ekins, 2015). Generation of energy via combustion of fossil fuel is the main source of CO_2 emission, thus depleting fossil fuel. The major challenge for adequate reduction of CO_2 emissions is disposing or utilizing the captured CO_2. A prospected and appealing method for utilizing captured CO_2 is CO_2 sequestration into biorenewable fuels or specialty chemicals (Jeong et al., 2012). Consequently, it is crucial to discover a renewable and sustainable energy source to alleviate the effect of global warming as well as meeting the rising energy need (Alaba, Sani and Daud, 2015a; Alaba et al., 2016a,b,c,d; Mikkelsen et al., 2010; Yui et al., 2011). Furthermore, researchers need to work extensively toward CO_2 storage and utilization to stabilize the atmospheric CO_2 level.

Theoretically, reduction of CO_2 emission in the atmosphere is mainly categorized into three routes, including CO_2 utilization, direct reduction of CO_2 emission, and CO_2 capture and storage (CCS) (Hurst et al., 2012; Windle and Perutz, 2012). Increasing industrialization (Alaba et al., 2016a,b,c,d; Bauer et al., 2013) combined with population growth cause the daily increase of fossil fuel consumption (Alaba et al., 2016a,b,c,d; Sani, Alaba, Raji-Yahya, Aziz and Daud, 2016a); therefore, the mitigation of CO_2 emission and the development of carbon-neutral renewable energy source appear unachievable. In addition, environmental hazard because of leakage, cost of gas compression, and transportation is the major disadvantage of the CCS (K. Li, An, Park, Khraisheh and Tang, 2014). Therefore, CO_2 reduction into fuels or specialty chemicals via major techniques, such as thermochemical, photochemical (Bai et al., 2015; Berardi et al., 2014; Qu and Duan, 2013), electrochemical (Back et al., 2015; Costentin et al., 2013; S. Ma and Kenis, 2013), inorganic transformation, (Sanna et al., 2014) and biological methods, is the growing concern of researchers since the past decade.

As commercially available CH_3OH from CO_2 technology uses Cu/Zn-based formulation and Cu/Zn/Al/Zr-based catalysts the catalysts should be improved. CO_2 is a stable compound and thus requires a substantial energy and highly stable and active catalyst for conversion into specialty chemicals. This finding requires developing suitable catalysts and intensifying CO_2 conversion for economical production. The techniques, prospects of the synthesis, and material and reactor design of using CO_2 as the main starting material for an economically viable renewable and sustainable energy source are investigated. The basic catalytic reduction of CO_2 is discussed first. The rational design of catalysts with remarkable activity as well as the critical factors for efficient catalytic reduction of CO_2 is emphasized. The progress in using CO_2 reduction catalytic reactors for clean fuel and specialty chemicals production is also discussed.

2. CO_2 reduction and its mechanism

In recent time, atmospheric CO_2 utilization engendered the replacement of CO with CO_2 as a feedstock for CH_3OH synthesis. The process is necessary to alleviate the GHG effect associated with considerable rise in the amount of CO_2 in the atmosphere (Olah, 2004; C. Yang et al., 2006). Catalytic reduction of CO_2 to CH_3OH is a remarkable approach toward green environment. Generally, CH_3OH synthesis from CO_2 starts in hydrogenation using suitable hydrogenation catalyst at temperature above 413 K and pressure above 1 MPa (J. Ma et al., 2009). When CO_2 is activated at high temperature and pressure for hydrogenation, the desired reaction

is CH_3OH production Eq. (1). Side reactions, such as reverse water-gas-shift (RWGS) reaction Eq. (2) and secondary reaction (3), which produces CO as an intermediate precursor, also occur (Qi et al., 2001a,b).

$$CO_2(g) + 3H_2(g) \rightarrow CH_3OH(g) + H_2O(g),\ \Delta H_{298\ K} = -49.47\ kJ/mol,\ \Delta G_{298\ K} = 3.30\ kJ/mol \quad (1)$$

$$CO_2(g) + H_2(g) \rightarrow CO(g) + H_2O(g),\ \Delta H_{298\ K} = 41.17\ kJ/mol,\ \Delta G_{298\ K} = 28.64\ kJ/mol \quad (2)$$

$$CH_3OH(g) \rightarrow CO(g) + H_2(g),\ \Delta H_{298\ K} = 90.64\ kJ/mol,\ \Delta G_{298\ K} = 25.34\ kJ/mol \quad (3)$$

The RWGS reaction consumes extra hydrogen, reduces CH_3OH production, and increases the amount of water produced. RWGS side reaction is detrimental to the active sites of the catalysts culminating in deactivation (Inui and Takeguchi, 1991). Furthermore, the formation of CO is engendered by catalysts with strong active site and long reaction time, which allows the decomposition of the primarily produced CH_3OH. Meanwhile, the strength of the active sites and reaction time favor hydrogenation of the CO produced from the RWGS reaction. Qi et al. (2001a,b) studied the selectivity of CH_3OH relative to the selectivity of CO by varying the contact time over Ti modified $CuO/\gamma -Al_2O_3$ catalyst (Fig. 1). They observed that CH_3OH selectivity increases while CO selectivity decreases with the increase in gas hourly space velocity (GHSV); low GHSV requires longer time between catalyst surface and reacting gas. Consequently, CH_3OH decomposition or hydrogenation of CO_2 (Eq. (3)) is a significant process. Liang et al. (2015) verified the effect of GHSV.

Furthermore, in the presence of solid acid catalyst, the CH_3OH formed in Eq. (1) is dehydrated to form dimethyl ether (DME) as follows (Jun et al., 1998; Shen et al., 2000; A. Xu et al., 2005; Gi-Won et al., 1999):

$$2CH_3OH(g) \leftrightarrow CH_3OCH_3\ (g) + H_2O(g),\ \Delta H_{298\ K} = -5.60\ kJ/mol \quad (4)$$

The overall reaction gives

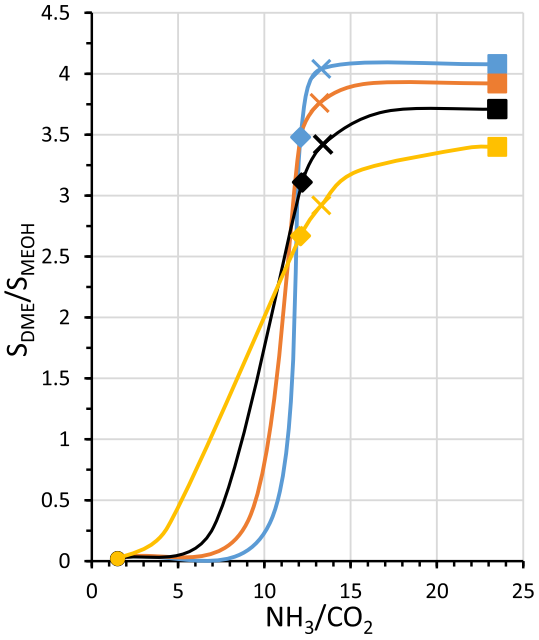

Fig. 2. Fitting of DME-to-MeOH selectivity ratio (SDME/SMeOH) as a function of NH3-to-CO2 chemisorption ratio: ■ZZ-CC; ×ZZ-NC; ●ZZ-OC; ◆ZZ-UH (Frusteri et al., 2015).

$$2CO_2(g) + 6H_2(g) \leftrightarrow CH_3OCH_3\ (g) + H_2O(g),\ \Delta H_{298\ K} = -29.40\ kJ/mol \quad (5)$$

Frusteri et al. (2015) prepared a series of Cu–ZnO–ZrO_2/H-ZSM-5 multifunctional catalysts by using different precipitating agents for direct conversion of CO_2 to DME via coprecipitation of CH_3OH catalyst with H-ZSM-5. They claimed that the functionality of hydrogenation of CO_2 to DME is related to a "multisite" reaction pathway, which involves combination of surface sites essential for the primary formation of CH_3OH. At the same time, H_2 is adsorbed/activated on the Cu sites and CO_2 on the strong basic sites (Fig. 2). Dehydration to DME occurs on acid sites of the H-ZSM-5.

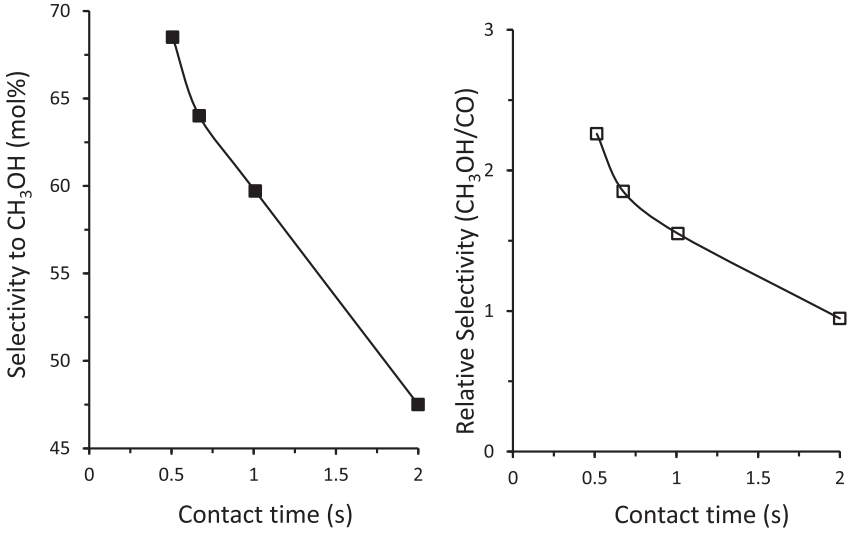

Fig. 1. Effect of contact time on selectivity to methanol and relative selectivity on CO2 hydrogenation. Relative selectivity: $\kappa = \chi(CH3OH)/\chi(CO)$ (χ = molar fraction). Reaction conditions: T = 240 °C, P = 3.0 MPa, CO2/H2 = 1/3 (molar ratio) (Qi et al., 2001a,b).

However, CO_2 reforming occurs at low pressure, high temperature, and H_2/CO_2 ratio greater than 3 (Kim et al., 2001) in the reacting gas mixture over supported noble metal catalysts such as Rh, Ru, Ir, Pd, and Pt (Szailer et al., 2007), with CH_4 as a by-product.

$$CO_2(g) + 4H_2(g) \leftrightarrow CH_4(g) + 4H_2O(g),\ \Delta H_{298\ K} = -113\ kJ/mol \quad (6a)$$

Therefore, rationally designing a catalyst with high selectivity for CH_3OH to circumvent formation of unwanted byproducts is vital.

The main components of the catalysts for hydrogenation of CO_2 are Zn and Cu, which are rationally incorporated into various modifiers such as oxides of Ti, Zr, Si, Ga, Al, Cr, B, V, and Ce (Arena et al., 2007; Liaw and Chen, 2001; Saito and Murata, 2004). CO_2, aided by hydrogen, dissociatively adsorbs on noble metals. The chemisorptions of CO_2 on supported Ru, Rh, and Pd catalysts in a hydrogenation process initiate the formation of surface metal hydride complex (Olah and Molnar, 2003). The characteristic atomic composition of commercially available CO_2 hydrogenation catalyst is 20–50% ZnO, 50–70% CuO, and 5–20% Al_2O_3.

Several authors studied the pathway to CH_3OH formation via CO_2 hydrogenation over catalysts such as $Cu/ZrO_2/SiO_2$ (Fisher and Bell, 1997, 1999) and Cu/ZnO (Huo et al., 2012). Huo et al. (2012) investigated the mechanism for the synthesis of CH_3OH from CO_2 hydrogenation over Cu/ZnO under hydrothermal condition. The proposed mechanism is presented in Fig. 3. They reported that ZnO absorbed CO_2, whereas hydrogen spilled over Cu. The absorbed CO_2 underwent a stepwise hydrogenation using the spilled hydrogen to form methoxide species on the ZnO. Furthermore, the methoxide species was hydrolyzed to CH_3OH and water as a co-product.

CO_2 dissociation stimulated by hydrogen, dissociation of surface metal hydride complex into reactive surface carbon, and hydrogenation of reactive surface carbon are the proposed steps in the hydrogenation process (Ravanchi and Sahebdelfar, 2014). Tabatabaei et al. (2006) investigated the co-adsorption of CO_2/H_2 gas mixture at 453 and 600 K onto the ZnO catalyst. They reported that at 453 K, the adsorbed CO_2/H_2 forms a formate species, which desorbs completely to H_2 and CO_2 at 530 K. The adsorbed CO_2/H_2 at 600 K forms formate species, which largely desorbs to CO and H_2 at 560 K with a trivial quantity of CO_2 and H_2 at 530 K. The formate (HCO_2^-) adsorbed on the ZnO catalyst was formed by the reaction

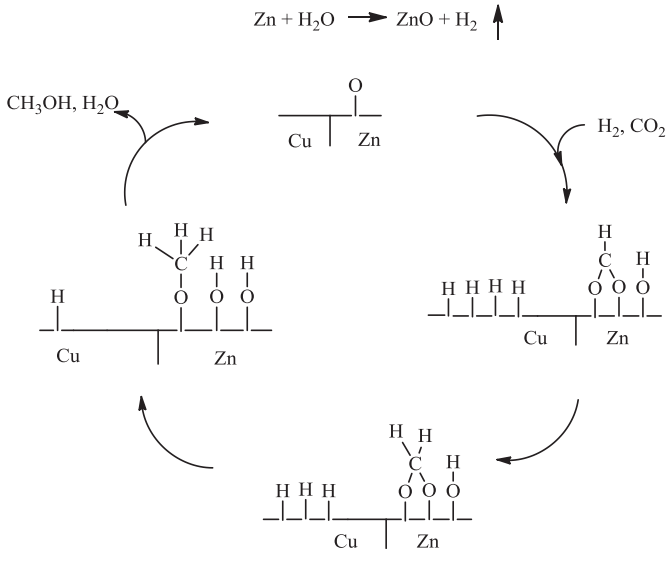

Fig. 3. Proposed pathway for the formation of methanol from CO2 hydrogenation over Cu/ZnO (Huo et al., 2012).

between the adsorbed H atom and the adsorbed CO_2 species. Structure 1 illustrates the bonding of H atom to a species of Zn^+ and bonding of CO_2 to the electron trapped at the anion vacancy on the terminal surface of Zn^+. This formate bonded monodentate at an anion vacancy was labelled as Vo-formate. The Vo-formate desorbed as CO and $1/2H_2$. Previously, Shido and Iwasawa (1993) reported the formation of bidentate formate from the interaction of an adsorbed bidentate carbonate with an adsorbed H atom. About 70% of the adsorbed bidentate formate desorbed to CO_2 and H_2. Tabatabaei et al. (2006) observed that the same adsorbed bidentate formate desorbed at 530 K as CO_2 and H_2. The formation of bidentate formate on Zn-terminated ZnO (0001) face is illustrated in Structure 2.

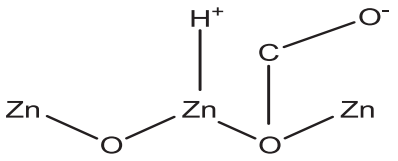

Structure 1.

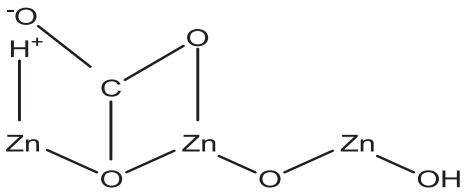

Structure 2.

Based on these findings, resources and operating conditions should be utilized in a suitable manner to make CO_2 hydrogenation process highly efficient, as CO_2 molecules are thermodynamically stable (Cuéllar-Franca and Azapagic, 2015; Zangeneh et al., 2011).

3. Metal oxide catalyst for CO_2 reduction

Supported metal catalysts play a vital role in CO_2 reductions. Suitable catalyst formulation facilitates interactions between CO_2 and a substrate on transition metal center M. Surprisingly, CO_2 exhibits a wide range of coordination and reaction modes in its homo- and polynuclear metal hydride complexes (Ravanchi and Sahebdelfar, 2014). Activation of CO_2 starts by inserting CO_2 into extremely reactive M–X bonds, leading to formation of new C–X bonds.

The reactions are usually stimulated by the nucleophilic attack of X at the Lewis acidic sites and C atom of CO_2 (Hu et al., 2013).

3.1. Transitional metal-based catalysts

Transition-metal oxides are active base metals commonly utilized as both catalysts and catalytic supports in various reactions. Prominent of all transition metals in CO_2 hydrogenation are Cu, Zn, Co, and Ni. The conventional catalyst for CO_2 hydrogenation is $CuO/ZnO/Al_2O_3$, but the reaction is usually followed by unwanted CO formation via the RWGS (Kunkes et al., 2015). Suppressing CO formation engendered the search for an optimal catalyst formulation to produce an efficient fuel from CO_2. Several researchers tried this approach via Cu-based catalysis (Q.-J. Hong and Liu, 2010; Jiang et al., 2015; Le Valant et al., 2015; Tisseraud et al., 2015; Y. Yang, Mims, Mei, Peden and Campbell, 2013; Yin and Ge, 2012).

(Le Valant et al., 2015) prepared a Cu–ZnO synergy by mechanical mixtures of varying Zn composition. The catalytic activity of the samples was investigated. The catalyst activity for CH_3OH yield versus Zn composition produced a volcano-like profile, which is a characteristic of the Cu–ZnO synergy with 100% CH_3OH selectivity. Furthermore, comparative study was done using coprecipitation and core-shell method. Core–shell catalysts (CuZn@ZnOx and Cu@ZnOx) give 100% CH_3OH selective, whereas coprecipitated catalyst (Cu–ZnO) favors high selectivity of CO resulting from RWSG reaction. The remarkable performance of the core–shell catalysts is due to metal ion migration, which allowed the formation of ZnOx active sites responsible for high CH_3OH selective. The findings of Tisseraud et al. (2015) also verified the remarkable activity of the core–shell catalysts.

In addition, the bimetallic catalysts combine the effect of the hydroxyls on the substrate with that of the alloyed metals to suppress CO formation. Yin and Ge (2012) investigated the effect of Cu addition to γ-Al_2O_3 supported CO. They reported that introduction of Cu to supported CO catalyst reduces the oxidation state of the metal cluster, leading to reduction in the activation barrier for formate formation by 0.36 eV. Activation barrier toward CO formation virtually remains constant. The report of Huo et al. (2012) confirmed the potency of bimetallic catalyst, suggesting that Zn acted as a reductant whereas Cu acted as the main catalyst for CO_2 hydrogenation in mild hydrothermal conditions.

3.2. Noble metal-based catalysts

Several researchers utilized noble metal-based catalysts such as Pd, Ru, Rh, and Pt for hydrogenation of CO_2 to biorenewable fuel (Back et al., 2015; Liang et al., 2015; Song et al., 2015). Prominent among the noble metal-based catalysts is Pd because of its considerable performance, including CH_3OH selectivity depending on the supports used (Mohammed et al., 2016; Shen et al., 2001; J. Xu et al., 2016). Liang et al. (2015) studied the performance of Pd-based catalyst by incorporating Pd-decorated carbon nanotubes into Pd/ZnO host. They reported that the catalysts demonstrated a remarkable performance toward hydrogenation of CO_2 to CH_3OH.

The recent study of (J. Xu et al., 2016) showed that Pd-based catalyst, modified by ZnO and promoted by Al_2O_3, gives a remarkable CH_3OH selectivity. They stressed that both Pd modified by ZnOx islands and PdZn alloy are viable active sites for CO_2 hydrogenation to produce CH_3OH. The pretreatment techniques and preparation methods have a significant effect on CH_3OH selectivity. The catalyst synthesized by deposition/precipitation techniques and wet impregnation exhibited lower CH_3OH selectivity than those obtained from coprecipitation technique.

The loading of Pd also plays a vital role in the performance of the Pd-based catalysts. According to Song et al. (2015), low CO_2 conversion, low CH_3OH selectivity, and high CO selectivity were obtained at Pd loading of 2%. Low Pd loading causes insufficient active sites, which cannot keep the formate to H_2 ratio equilibrated. Increase in Pd loading from 2% to 6% leads to increase in conversion of CO_2 and selectivity toward CH_3OH and CH_4 as well as decrease in selectivity to CO (Fig. 4). However, further increase in Pd loading (up to 8%) rapidly decreases the selectivity of CH_3OH and CH_4, whereas the selectivity of CO and conversion of CH_3OH increases. Poor activity of the 8% Pd loading is attributed to the increase in CaO loading and decrease in the dissociation of the H_2 spilt over the Pd active sites, resulting in less active H_2 for hydrogenation of the formate formed on the surface of CaO, hence the high selectivity of CO and low selectivity of CH_3OH.

3.3. Transitional metal carbides catalysts

The Lewis acidity of some transition-metal oxides with high oxidation state poses a major setback for their use in CO_2 hydrogenation (Borodko and Somorjai, 1999). CO_2 reduction with these transition-metal oxides leads to prevalent hydrogenation of formate to CH_4 rather than CH_3OH. The oxidation state of these transition-metal oxides can be reduced by transformation to transitional metal carbides (TMCs). TMC is a metal compound obtained by incorporating carbon in the metal lattice through carbothermal reduction (Tuomi et al., 2016). The process improves the metal compound's physico-chemical properties, such as melting point, hardness, thermal and mechanical stability, and adsorption capacity (Jongerius et al., 2013; Porosoff et al., 2014; Qi et al., 2001a,b; Tominaga and Nagai, 2005). The improvement engenders remarkable catalytic performance for several reactions including CO_2 hydrogenation (Chen et al., 2015, 2016; Dubois et al., 1992; W. Xu, Ramirez, Stacchiola and Rodriguez, 2014), CH_4 reforming (Setthapun et al., 2008), and water–gas shift (Schweitzer et al., 2011), similar to the activities of noble metals such as Pt, Pd, Ru, and Rh (J. Ma et al., 2009). Several TMCs, such as WC, Mo_2C, and Fe_3C, are active catalysts for CO_2 hydrogenation (Dubois et al., 1992). Dubois et al. (1992) reported that hydrogenation of CO_2 over Fe_3C and Mo_2C gives high CO_2 conversion and remarkable CH_3OH selectivity at 493 K. They also claimed that the use of WC favors selectivity toward DME. In addition, SiC and TaC are poor CO_2 hydrogenation catalysts. Tominaga and Nagai (2005) also reported better performance of Mo_4C_2 for CO_2 hydrogenation because of its improved adsorption capacity, as compared with Mo_2.

TMCs are also effective co-catalysts and support to alcohols and hydrocarbons in low-temperature CO_2 hydrogenation. Chen et al. (2016) studied the use of Mo_2C in Pd- and Cu-based catalysts for CO_2 hydrogenation. They reported that addition of Cu/Mo_2C and Pd/Mo_2C exhibits higher selectivity toward CH_3OH compared with Mo_2C, whereas Co/Mo_2C and Fe/Mo_2C showed improved selectivity toward C^{2+} hydrocarbons (Table 1). The supported TMC catalysts exhibit high hydrothermal stability.

4. Important factors for catalytic reduction of CO_2

Several important factors determine the reactants' residence time in the reactor and consequent catalytic activity. The conversion of CO_2 and selectivity of CH_3OH are determined by thermodynamic equilibrium values particular to catalyst formulation. The important factors are temperature, pressure, GHSV, and H_2/CO_2 ratio.

4.1. Effect of H_2/CO_2

Generally, increase in the H_2/CO_2 ratio favors CO_2 conversion, whereas the CO selectivity declines. Furthermore, increasing the H_2/CO_2 ratio favors CH_4 selectivity. Kim et al. (2001) reported that the optimum value of H_2/CO_2 ratio is ~3 because the selectivities of unwanted products, such as paraffin and CH_4, increase as H_2/CO_2 increases. However, Bansode and Urakawa (2014) proved that increase in H_2/CO_2 ratio above 3 largely reduces the CO formation without producing unwanted products (Fig. 5). This finding is due to the use of high pressure (36 MPa).

4.2. Temperature and pressure

Temperature and pressure have a significant influence on reactions in gaseous state. Increase in temperature and pressure

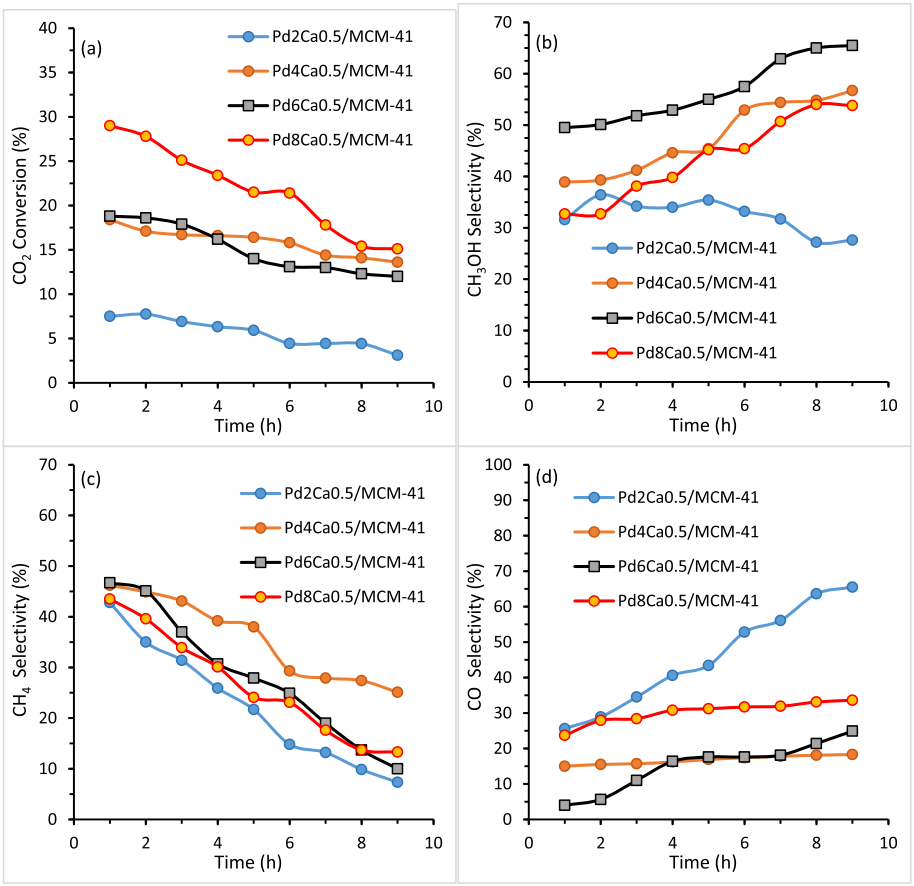

Fig. 4. Reactivity of CO_2 hydrogenation and selectivity for different products over the $PdxCa_{x/2}$/MCM-41 (Song et al., 2015).

elevates the concentration of the reactants and the collision speed of the particles, resulting in increased reaction rate. Several researchers investigated the effect of temperature on the catalytic activity in CO_2 hydrogenation (Kunkes et al., 2015; M. M.-J. Li, Zeng, Liao, Hong and Tsang, 2016; Qi et al., 2001a,b; Y. Yang et al., 2013). The yield of CH_3OH increases as the temperature increases; however, the yield starts to decrease with temperature elevation when the system reaches its thermodynamic limit, signifying the limiting behavior of the system (M. M.-J. Li et al., 2016). The thermodynamic limit of the reaction solely depends on the catalyst used (Fig. 6). Temperature also plays a vital role on selectivity of the desired product based on catalyst formulation. Lachowska and Skrzypek (2004) studied the effect of temperature in CO_2 hydrogenation using various formulation of Mn-promoted Cu/Zn/Zr catalysts. They reported that all the samples, irrespective of their formulation, exhibited increase in CH_3OH yield as the temperature is raised. However, the formulation with 5.6 wt% ZrO_2 and 2 wt% MnO gives the highest yield and selectivity (91%) of CH_3OH, whereas the formulation with 3.6 wt% ZrO_2 and 4 wt% MnO gives 100% selectivity with conspicuously lower yield of CH_3OH.

Several findings verified the positive influence of pressure on catalytic CO_2 hydrogenation (Gaikwad et al., 2016; Kim et al., 2001; Lachowska and Skrzypek, 2004; Tidona et al., 2013). The effect of both temperature and pressure on conversion of CO_2 and selectivity of CH_3OH was extensively studied by Gaikwad et al. (2016). They emphasized the significance of high operating pressure based on thermodynamic computations (Fig. 7, dotted lines). Experimentally, they reported that CO_2 conversion and CH_3OH selectivity increase

Table 1
Performance of transitional metal carbides (TMCs) catalysts.

Catalyst	T/P K/MPa	H_2/CO_2	TOF (s-1×10^4)	CO_2 Conv. (%)	Selectivity (%)					Ref.
					MEOH	EtOH	CH_4	CO	C_{2+}	
Mo_2C	200/4	3	20	55	53	16	17	5	8.8	(Chen et al., 2016)
	135/4	3	0.6	1.7	79		5.3	16		(Chen et al., 2016)
Cu/Mo_2C	200/4	3	41	90	62	14	10	9	5.9	(Chen et al., 2016)
Fe/Mo_2C	200/4	3	38	99	58	16	8	7	10.5	(Chen et al., 2016)
Pd/Mo_2C	200/4	3	39	97	68	11	7.6	9.6	4.1	(Chen et al., 2016)
Co/Mo_2C	200/4	3	35	86	46	25	9.5	9.5	7.6	(Chen et al., 2016)
α-MoC_{1-x}	200/2	5	14	3	28	1	11	52	5	(W. Xu, Ramirez, Stacchiola and Rodriguez, 2014)
β-MoC_y	200/2	5	106	6	21	1	29	39	8	(W. Xu et al., 2014)
Cu/Mo_2C	220/6	0.33	219	4	32	0.4	14	49	4	(Dubois et al., 1992)

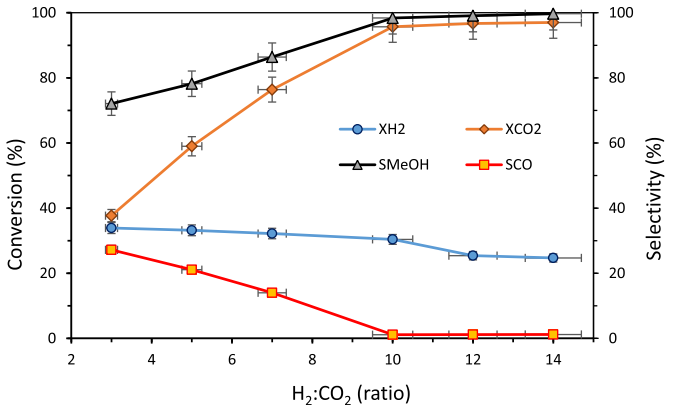

Fig. 5. Effects of the CO_2/H_2 feed ratio on CO_2 conversion (XCO_2), H2 conversion (XH2) and selectivity to CO (SCO), and methanol (SMeOH) in CO_2 hydrogenation over the Cu/ZnO/Al_2O_3 catalyst. Reaction conditions: T = 260 °C, P = 36 MPa, GHSV = 10,471 h^{-1} (Bansode and Urakawa, 2014).

with pressure. At 300 °C, the conversion increased from 25.1% to 81.7%, whereas the selectivity increased from 13% to 93.1% as the pressure is raised from 46 bar to 442 bar (Fig. 7). Lachowska and Skrzypek (2004) also showed that pressure elevation increases the yield of CH_3OH.

4.3. Effect of space velocity

Several studies revealed that GHSV plays a vital role in the catalytic reduction of CO_2 (Gaikwad et al., 2016; Lachowska and Skrzypek, 2004). The selectivity of CH_3OH increases whereas CO selectivity decreases with the increase in GHSV, because low GHSV requires longer time between the surface of the catalyst and the reacting gas. Therefore, increase in GHSV favors the yield and selectivity of the desired products (Lachowska and Skrzypek, 2004; Lee et al., 2000). However, when the catalytic activity reaches the thermodynamic limit, further increase in GHSV will decrease (little or no effect) the performance of the catalytic activity (Gaikwad et al., 2016) (Fig. 8). This finding is traceable to the occurrence of side reaction, leading to the formation of ethanol and ethane.

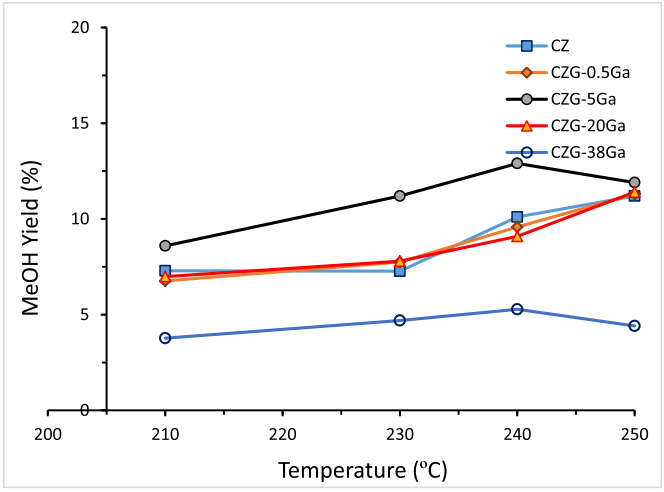

Fig. 6. Methanol yield of CO2 hydrogenation reaction over CZ and CZG samples prepared with various chemical compositions (all calcined at 330 °C) (Li et al., 2016).

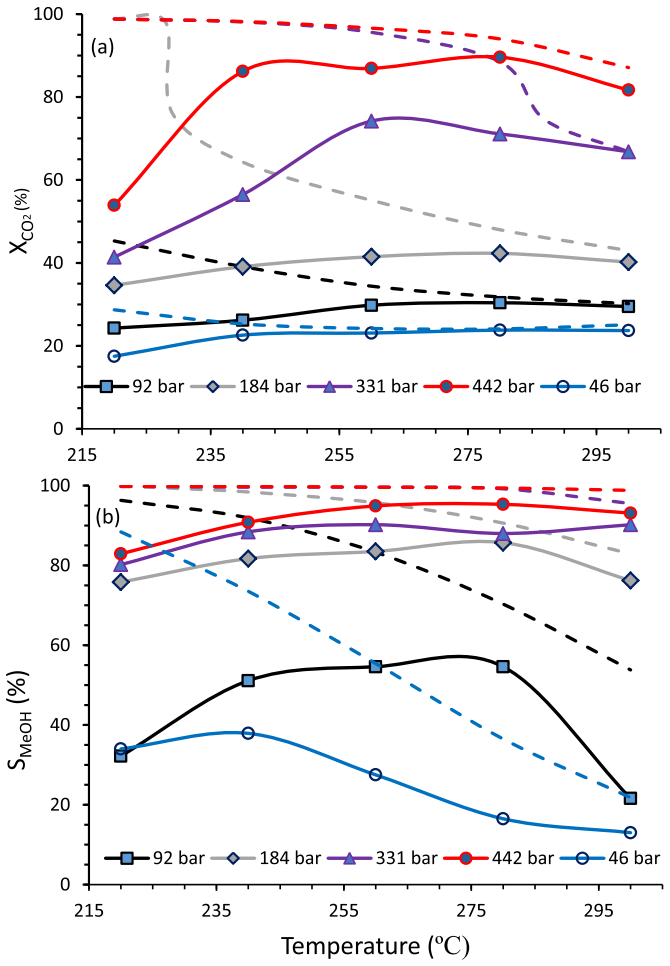

Fig. 7. Effects of reaction temperature and pressure on CO2 conversion (X_{CO2}) (a) and methanol selectivity (S_{MeOH}) (b) in high-pressure stoichiometric CO_2 hydrogenation using commercial $Cu/ZnO/Al_2O_3$ catalyst at constant GHSV of 10,000 h^{-1} (5.87 NL $gcat^{-1}$ h^{-1}). Dotted lines show the theoretical equilibrium CO_2 conversion and methanol selectivity (Gaikwad et al., 2016).

5. Influence of promoter on CO_2 reduction

The catalytic properties of solid catalysts can be improved by adding small quantities of promoters (Fujitani et al., 1995; Koizumi et al., 2012; Natesakhawat et al., 2013; Oyola-Rivera et al., 2015). However, the outcome and operation method of promoters are quite vague, thereby hindering the rational optimization of the materials (Behrens et al., 2013; Bonura et al., 2013; L. Li, Mao, Yu and Guo, 2015). Although CO_2 is kinetically and thermodynamically stable and is hardly utilized to its full potential, this chemical compound is an anhydrous carbonic acid, which quickly interacts with basic oxides. This characteristic entails that CO_2 exhibits a strong attraction to nucleophiles and electron-donors because of carbonyl carbons electron deficiency (Prieto et al., 2013; Sakakura et al., 2007). Metal oxide promoters enhance the dispersity of metal oxide catalysts leading to improved pressure swing adsorption (PSA) of the synthesis gases. Furthermore, the promoters stabilize the adsorbed CO_2 and the produced formate adsorbed on the catalyst, whereas the supported metal catalysts dissociate molecules of H_2 (Gotti and Prins, 1998).

Several suitable promoters such as Cr_2O_3, ZrO_2, Al_2O_3, CaO, K_2O, CeO_2, Ga_2O3, La_2O_3, and CNTs are used for CO_2 hydrogenation (Behrens et al., 2013; Z.-s. Hong, Cao, Deng and Fan, 2002; Liang

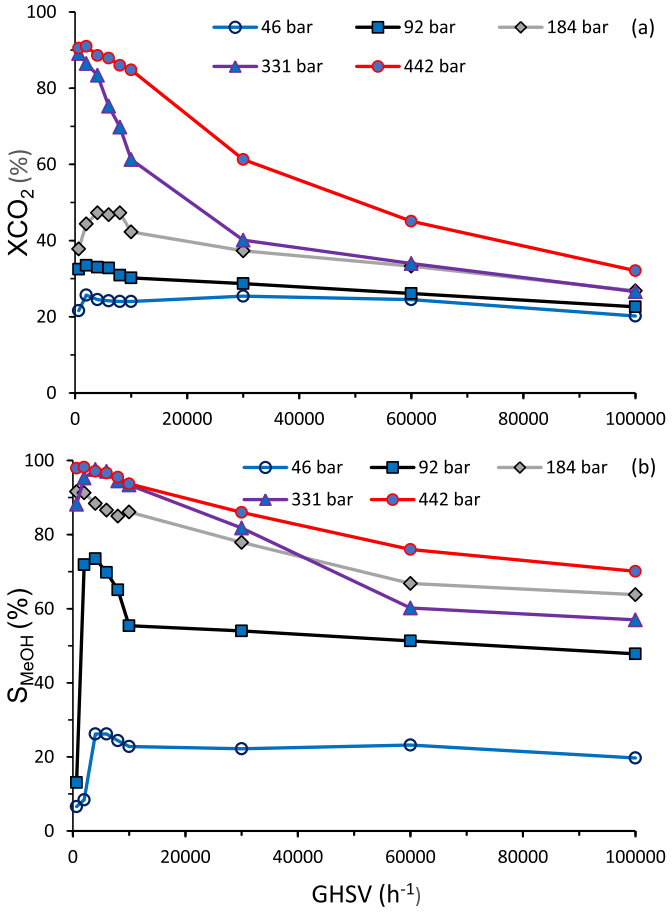

Fig. 8. CO_2 conversion (X_{CO2}) (a) and methanol selectivity (S_{MeOH}) (b) in high-pressure stoichiometric CO_2 hydrogenation at different GHSV conditions (650–100,000 h^{-1}) at 280 °C (Gaikwad et al., 2016).

et al., 2015; Song et al., 2015; Wang et al., 2002). Behrens et al. (2013) claimed that these compounds promote the catalysts both structurally and electronically.

(Song et al., 2015) reported the influence of acid–base properties of metal oxides by analyzing the effect of incorporating CaO, La_2O_3, K_2O, and Ga_2O_3 to Pd/MCM-41 catalyst. They claimed that both Pd_4-Ca_2O/MCM-41 and Pd_4-La_2O_3/MCM-41 improve CH_3OH selectivity and CO_2 conversion, whereas lower CH_4 and CO selectivity was experienced with Pd4-Ca_2O/MCM-41. This finding is due to the fact that CaO is an alkali earth metal oxide possessing moderate basic strength and is capable of adsorption and activation of CO_2 on the metal oxide surface, thereby increasing formate on the catalyst surface. Consequently, the hydrogenation of formate to CH_3OH was boosted (Song et al., 2015). Meanwhile, the use of Pd_4-K_2O/MCM-41 or Pd_4-Ga_2O_3/MCM-41 lowers CH_3OH selectivity and CO_2 conversion, whereas improved CO selectivity was experienced with Pd_4-K_2O/MCM-41 because K_2O is a strong base. The presence of K_2O stimulates unnecessary stabilization of the formate intermediate, leading to its decomposition to CO. Fig. 9 illustrates the mechanism of CO_2 hydrogenation with CaO-promoted Pd catalyst. Furthermore, Pd4-Ga_2O_3/MCM-41 shows lower selectivity toward CH_4 selectivity because of the Ga_2O_3 Lewis acid properties (Collins et al., 2002), which favors hydrogenation of formate to CH_4. Therefore, promoters with high cation electronegativity are considered modest promoters. Metal oxides with moderate basic strength or amphoteric properties are considered excellent promoters (Nomura et al., 1998), as these compounds enhance the hydrophobicity of the catalyst leading to better activity.

(Liang et al., 2015) reported that CNTs as promoter to Pd-based catalyst performed excellently by providing adsorption/activation of H_2 to the sp^2-C surface sites to form a surface micro-environment with an improved amount of stationary-state, H-adsorbed species in the form of sp^2-C-H on catalyst surface. The process terminated in a notable rise of the Pd^0-species surface concentration in the form of PdZn alloys, a catalytically active Pd^0-species linked to the production of CH_3OH.

Bimetallic support plays a synergistic effect in CO_2 hydrogenation of enhanced CH_3OH selectivity (An et al., 2007; Bahruji et al., 2016; Liang et al., 2009; Liu et al., 2005; Toyir, de la Piscina, Fierro and Homs, 2001). Jiang et al. (2015) proved that the formation rate of methanol over Pd(0.25)–Cu/SiO_2 was remarkable. Both Cu/Pd and Pd/Cu catalysts exhibited similar activities and were more active than monometallic Cu and Pd catalysts (Table 2). Table 2 also presents the influence of several promoters on the synthesis of CH_3OH.

6. Development of CO_2 reduction reactor and process intensification

Developing CO_2 reduction reactor is an engineering technique for enhancement of CO_2 hydrogenation efficiency. The technique includes improvement on rational design of catalysts for a remarkable conversion; understanding the reaction kinetics; improved yield and selectivity of the desired product; reduction of byproduct formation; and improvement on product separation.

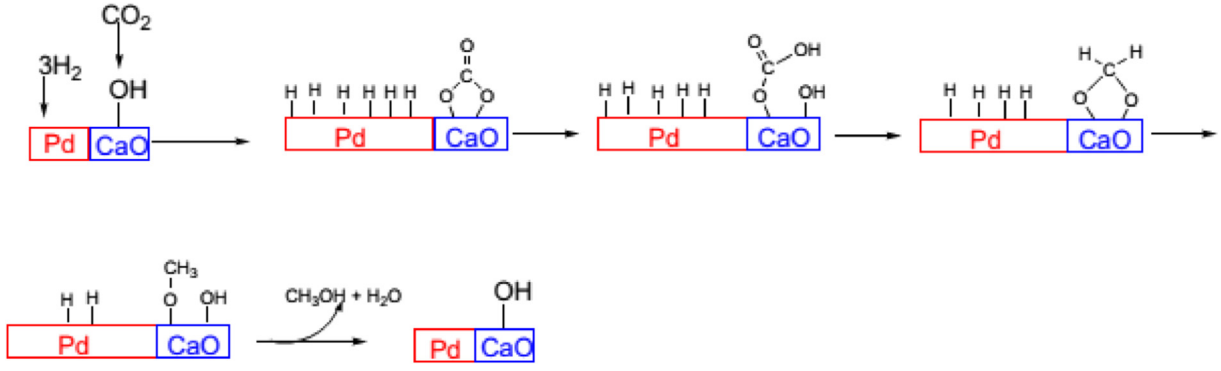

Fig. 9. Mechanism of hydrogenation of CO_2 in the presence of CaO as a promoter (Song et al., 2015).

Table 2
Effect of promoter on the Synthesis of Methanol.

Catalyst	Reactor	Temp. K	Press. MPa	GHSV L/h	CO_2 conv %	Selectivity (%)				Ref.
						MEOH	DME	CH_4	CO	
Fe-Cu-K-Al	Fixed bed	573	1		32.3			8.5	11.0	(Kim et al., 2001)
Fe-Cu-K-Al	Fluidized bed	573	1		46.8			9.2	14.5	(Kim et al., 2001)
CuZnZrGaY	Fixed bed	453	2	30		90			10	(Natesakhawat et al., 2013)
Cu/ZnO/Al2O3	Fixed bed	513	2	3600	20.1	31.3				(Hong et al., 2002)
Cu/ZnO/Al2O3	Fixed bed	513	2	7200	17.3	32.4				(Hong et al., 2002)
CuO/SiO2-A1203	Stainless steel	513	1		1.4	17.3			48.1	(Nomura et al., 1998)
CuO/SiO2	Stainless steel	513	1		0.6	0.0	34.6		100	(Nomura et al., 1998)
CuO/MgO	Stainless steel	513	1		1.8	7.5	0.0		92.5	(Nomura et al., 1998)
CuO/A1203	Stainless steel	513	1		3.6	10.0	0.0		76.0	(Nomura et al., 1998)
CuO/A1203	Stainless steel	543	1		10.6	5.5	6.4		88.1	(Nomura et al., 1998)
CuO/ZrO2	Stainless steel	513	1		3.2	29.4	14.0		70.6	(Nomura et al., 1998)
CuO/TiO2	Stainless steel	513	1		3.2	42.5	0.0		57.5	(Nomura et al., 1998)
CuO-K20/TiO2	Stainless steel	513	1		8.2	5.6	0.0		94.4	(Nomura et al., 1998)
CuO-B2O3/TiO2	Stainless steel	513	1		2.8	34.3	0.0		65.7	(Nomura et al., 1998)
CuO-B2O3/Al2O3	Stainless steel	543	1		6.4	7.6	11.6		80.8	(Nomura et al., 1998)
CuO-P205/A1203	Stainless steel	543	1		3.2	4.7	10.9		84.4	(Nomura et al., 1998)
5CuAl	Continous flow	523	2.94			54.91		0.55	44.54	(Wang et al., 2002)
5CuCe20	Continous flow	523	2.94			71.94		0.09	27.97	(Wang et al., 2002)
5CuY5Ce20	Continous flow	523	2.94			78.69		0.03	21.28	(Wang et al., 2002)
5CuY10Ce20	Continous flow	523	2.94			83.68		0.03	16.28	(Wang et al., 2002)
5CuY15Ce20	Continous flow	523	2.94			84.69		0.08	15.22	(Wang et al., 2002)
5CuY20Ce20	Continous flow	523	2.94			85.60		0.04	14.36	(Wang et al., 2002)
5CuCe50	Continous flow	523	2.94			75.98		2.12	21.90	(Wang et al., 2002)
5CuY5Ce50	Continous flow	523	2.94			85.70		1.27	13.03	(Wang et al., 2002)
5CuY10Ce50	Continous flow	523	2.94			86.29		1.28	12.43	(Wang et al., 2002)
5CuY15Ce20	Continous flow	523	2.94			86.69		0.54	12.77	(Wang et al., 2002)
5CuY20Ce20	Continous flow	523	2.94			90.60		0.38	9.03	(Wang et al., 2002)
Cu/ZnO/ZrO2/Al2O3	Fixed bed	523	3		12.6	70			30	(Jeong et al., 2012)
Cu/ZnO/Al203		523	3	18,000	16.9	42.3		0.7	57.0	(Lee et al., 2000)
Cu/ZnO/Al203		523	3	54,000	7.0	65.2		1.0	33.7	(Lee et al., 2000)
Cu/ZnO/Al203		523	3	108,000	7.1	61.7		0.8	37.5	(Lee et al., 2000)
Cu/ZnO/Al203		523	3	73,000	13.5	61.8		0.6	37.6	(Lee et al., 2000)
Cu/Al–Ti(10)	high-pressure microreactor	453	3	3600	7.5	88.3			13.8	(Qi et al., 2001a,b)
Cu-Ti(10)/γ-Al2O3	Fixed bed	513	3	3600	23.0	59.3			38.1	(Qi et al., 2001a,b)
Cu/Zn/Zr	Fixed bed	493	8	3400		88.0			12.0	(Lachowska and Skrzypek, 2004)
Mn-promoted Cu/Zn/Zr	Fixed bed	493	8	3400		91.0			9.0	(Lachowska and Skrzypek, 2004)
Mn-promoted Cu/Zn/Zr	Fixed bed	493	8	3400		100.0			0.0	(Lachowska and Skrzypek, 2004)
Industrial CuO/ZnO/Al2O3	Fixed bed	493	8	3400		40.0			60.0	(Lachowska and Skrzypek, 2004)
5 wt% Pd/ZnO	Fixed bed	453	3	3600	2.5	72.2				(J. Xu et al., 2016)
5 wt% Pd/ZnO/Al2O3	Fixed bed	453	3	3600	2.9	79.4				(J. Xu et al., 2016)
Pd/SiO2	Fixed bed	523	4.1	3600	3.0	23			77	(Jiang et al., 2015)
Cu/SiO2	Fixed bed	523	4.1	3600	2.8	15			85	(Jiang et al., 2015)
Pd(0.25)–Cu/SiO2	Fixed bed	523	4.1	3600	6.7	30			70	(Jiang et al., 2015)
Pd(0.34)–Cu/SiO2	Fixed bed	523	4.1	3600	6.6	34			66	(Jiang et al., 2015)
Cu–Zn(0.67)/SiO2	Fixed bed	523	4.1	3600	2.2	50			50	(Jiang et al., 2015)
Pd(0.25)–Cu/MCM-41	Fixed bed	523	4.1	3600	6.2	23			77	(Jiang et al., 2015)
Cu/SBA-15	Fixed bed	523	4.1	3600	1.5	12			88	(Jiang et al., 2015)
Pd(0.25)–Cu/SBA-15	Fixed bed	523	4.1	3600	6.5	23			77	(Jiang et al., 2015)
Pd/MSU-F	Fixed bed	523	4.1	3600	<1	14			86	(Jiang et al., 2015)
Cu/MSU-F	Fixed bed	523	4.1	3600	<1	18			82	(Jiang et al., 2015)
Pd(0.25)–Cu/MSU-F	Fixed bed	523	4.1	3600	5.3	18			82	(Jiang et al., 2015)
Cu–ZnO–Al2O3	Fixed bed	523	4.1	3600	18.4	27			73	(Jiang et al., 2015)
Pd–Nb_2O_5/LSGa2O_2	Fixed bed	543	1.72	27[a]		60	40			(Oyola-Rivera et al., 2015)
Mg(0.5)/Pd(4)/SBA-15	Fixed bed	523	4.1		3	40			60	(Koizumi et al., 2012)
Ca(0.5)/Pd(4)/SBA-15	Fixed bed	523	4.1		7	31			69	(Koizumi et al., 2012)
Pd(4)/Ca(0.5)/SBA-15	Fixed bed	523	4.1		6	39			61	(Koizumi et al., 2012)
40%Cu/ZnO/Al2O	Fixed bed	523	4.1		17	36			64	(Koizumi et al., 2012)
CZ	Fixed bed	513	4.5		20	39.0			61	(M. M.-J. Li, Zeng, Liao, Hong and Tsang, 2016)
CZG-0.5Ga	Fixed bed	513	4.5		20.8	46.0			54	(M. M.-J. Li et al., 2016)
CZG-5Ga	Fixed bed	513	4.5		27.0	50.0			50	(M. M.-J. Li et al., 2016)
CZG-20Ga	Fixed bed	513	4.5		19.6	46.5			53.5	(M. M.-J. Li et al., 2016)
CZG-38Ga	Fixed bed	513	4.5		18.0	30.4			69.6	(M. M.-J. Li et al., 2016)
S-CZZ-300	Fixed bed	513	3	3600	12.1	54.1			45.9	(L. Li, Mao, Yu and Guo, 2015)
S-CZZ-400	Fixed bed	513	3	3600	11.0	55.4			44.6	(L. Li et al., 2015)
S-CZZ-500	Fixed bed	513	3	3600	9.3	58.9			41.1	(L. Li et al., 2015)
S-CZZ-600	Fixed bed	513	3	3600	4.8	73.4			26.6	(L. Li et al., 2015)

Table 2 (*continued*)

Catalyst	Reactor	Temp. K	Press. MPa	GHSV L/h	CO_2 conv %	Selectivity (%)				Ref.
						MEOH	DME	CH_4	CO	
CZZ-300	Fixed bed	513	3	3600	14.3	32.5			67.5	(L. Li et al., 2015)
CZZ-400	Fixed bed	513	3	3600	11.7	33.2			66.8	(L. Li et al., 2015)
CZZ-500	Fixed bed	513	3	3600	10.4	36.5			63.5	(L. Li et al., 2015)
CZZ-600	Fixed bed	513	3	3600	8.1	38.6			61.4	(L. Li et al., 2015)
Cu–ZnO–ZrO2/HZSM-5	Fixed bed	453	3	10,000	2.5	16.7	72.7		10.6	(Bonura et al., 2013)
Cu–ZnO–ZrO2/HZSM-5	Fixed bed	473	3	10,000	5.1	16.2	62.3		21.5	(Bonura et al., 2013)
Cu–ZnO–ZrO2/HZSM-5	Fixed bed	493	3	10,000	9.6	14.2	46.6		39.3	(Bonura et al., 2013)
Cu–ZnO–ZrO2/HZSM-5	Fixed bed	513	3	10,000	16.1	11.8	33.9		54.3	(Bonura et al., 2013)
Cu/SiO2 Impregnation	Stainless steel	533	4		15–20	98				(Prieto et al., 2013)
Cu/ZnO/Al2O3 Co-precipitation	Microreactor	533	36		37	72			28	(Bansode and Urakawa, 2014)
Pd/ZnO Co-precipitation	Flow reactor	523	5		13.8	37.5			62.5	(Fujitani et al., 1995)
Pd/ZnO/CNT Impregnation	Fixed bed	523	3		7.58	95			5	(Liang et al., 2009)
Cu/Zn/Ga/SiO2 Co-impregnation	Fixed bed	523	2		5.6	99.5			0.5	(Toyir, de la Piscina, Fierro and Homs, 2001)
Cu/Ga2O3/ZrO2 deposition precipitation	Fixed bed	523	2		13.71	75.6			24.4	(Liu et al., 2005)
Cu/Zn/Al/ZrO2 Co-precipitation	Fixed bed	513	4		18.7	47.2			52.8	(An et al., 2007)
5% Pd/ZnO sol immobilised, 393 K calcination	Fixed bed	523	2		10.7	60			39	(Bahruji et al., 2016)
5% Pd/ZnO sol immobilised, 523 K calcination	Fixed bed	523	2		10.8	60			39	(Bahruji et al., 2016)
5% Pd/ZnO sol immobilised, 673 K calcination	Fixed bed	523	2		11.1	59			40	(Bahruji et al., 2016)
5% Pd/ZnO impregnated, 393 K calcination	Fixed bed	523	2		8.7	2.17			97.8	(Bahruji et al., 2016)

[a] WHSV (h^{-1}).

6.1. Reaction kinetics

CO_2 hydrogenation proceeds over a hydrogenation catalyst according to kinetics proposed by (Graaf et al., 1988) (Eqs. (6)–(17)).

$$r_{H_2O,A} = \frac{k'_{ps,A} K_{CO_2}\left[f_{CO_2} f_{H_2} - f_{H_2O} f_{CO} \Big/ K^0_{p1}\right]}{\left(1 + K_{CO} f_{CO} + K_{CO_2} f_{CO_2}\right)\left[f_{H_2}^{1/2} + \left(K_{H_2O} \Big/ K_{H_2}^{1/2}\right) f_{H_2O}\right]} \tag{6b}$$

$$r_{CH_3OH,B} = \frac{k'_{ps,B}\, K_{CO_2}\left[f_{CO_2} f_{H_2}^{3/2} - f_{CH_3OH} f_{H_2O} \Big/ \left(f_{H_2}^{3/2} K^0_{p2}\right)\right]}{\left(1 + K_{CO} f_{CO} + K_{CO_2} f_{CO_2}\right)\left[f_{H_2}^{1/2} + \left(K_{H_2O} \Big/ K_{H_2}^{1/2}\right) f_{H_2O}\right]} = \left(r_{H_2O,B}\right) \tag{7}$$

where f_{CO}, f_{CO2}, and f_{H2} are the partial fugacities (in bar); K_{CO}, K_{CO2}, K_{H2O}, and $K_{H_2}^{1/2}$ are the adsorption constants in bar; and ${}^{-1}k'_{ps,A}$ and $k'_{ps,B}$ are the reaction rate constants, given by Eqs. (8)–(13), with activation energies in J/mol. The equilibrium constant K^0_{p1} (Eq. (14)) is obtained from (Graaf et al., 1986).

$$k'_{ps,A} = (7.31 \pm 4.9) \times 10^8 \; exp\left(\frac{-123,400 \pm 1,600}{RT}\right) \tag{8}$$

$$k'_{ps,B} = (4.36 \pm 0.25) \times 10^2 \; exp\left(\frac{-65,200 \pm 200}{RT}\right) \tag{9}$$

$$K_{CO} = (7.99 \pm 1.28) \times 10^{-7} \; exp\left(\frac{58,100 \pm 600}{RT}\right) \tag{10}$$

$$K_{CO_2} = (1.02 \pm 0.16) \times 10^{-7} \; exp\left(\frac{67,400 \pm 600}{RT}\right) \tag{11}$$

$$K_{H_2O} \Big/ K_{H_2}^{1/2} = (4.13 \pm 1.51) \times 10^{-11} \; exp\left(\frac{104,500 \pm 100}{RT}\right) \tag{12}$$

$$\log_{10}\left(K^0_{p1}\right) = \frac{-2,073}{T} - 2.029 \tag{13}$$

$$K^0_{p2} = K^0_{p1} \tag{14}$$

A rigorous process, such as microkinetics method covering a wide range of operating conditions, is more suitable to optimize the CO_2 hydrogenation reactor compared with traditional kinetic models. Microkinetics is a mean-field method that evaluates the reaction kinetics based on the catalyst activity, without intervention from external or internal transport effect (Mendes et al., 2014). However, the major disadvantages of this method includes the presence of fluctuations, surface heterogeneity, limited lateral interactions, and mobility of adsorbates used in some heterogeneous catalysis (Evans et al., 2002; Temel et al., 2007; Zhdanov, 2002). Moreover, the hypothesis of mean-field in microkinetics is ineffective for the reaction at the interface of the metal/oxide catalysts because the overall reaction rate is overrated (Q.-J. Hong and Liu, 2010).

Kinetics Monte Carlo (KMC) method is a more reliable approach for heterogeneous catalysis simulation as compared with the microkinetics approach. KMC simulations give a more profound understanding of complex interfacial catalysis provided by the reaction rate, activation energies, and products selectivity (Q.-J. Hong and Liu, 2010; Tang et al., 2009). Furthermore, KMC gives insight into the secondary reaction associated with readsorption of

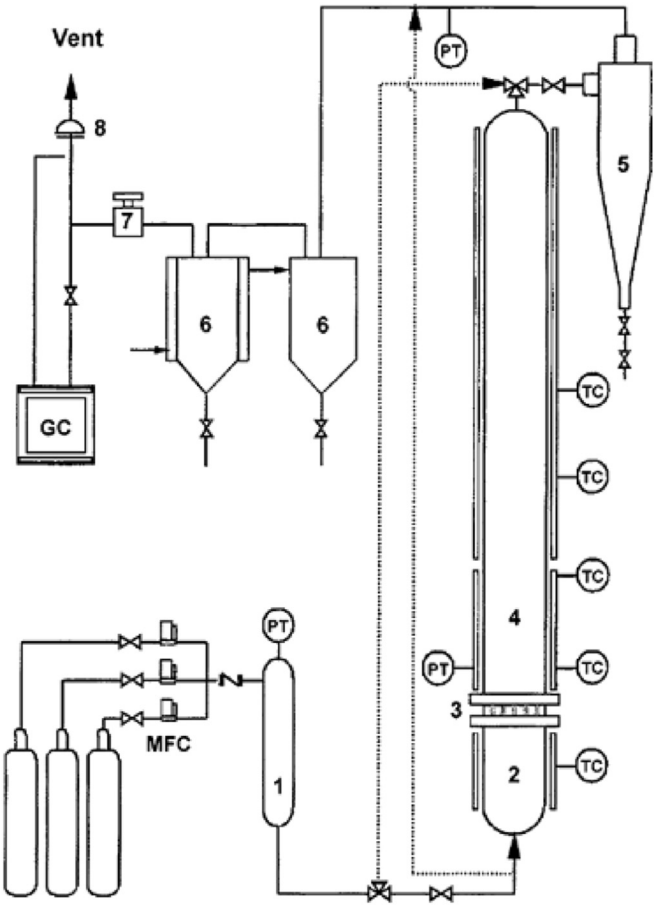

Fig. 10. Fluidized bed batch reactor setup for catalytic hydrogenation of CO2 (Kim et al., 2001).

products, which makes significant contribution to selectivity and reaction rate (Q.-J. Hong and Liu, 2010). Several authors studied the use of first principles KMC simulations in various systems (Neurock et al., 2004; Reuter et al., 2004; Sendner et al., 2006). KMC simulations are capable of dealing with complex reaction process with high precision relative to the experiments. Q.-J. Hong and Liu (2010) studied DFT-based KMC on the mechanism of CO_2 conversion on the interface of Cu/ZrO_2. They reported that CO was predominantly produced along with CH_3OH through the formate pathway than RWGS. In determining the free energy profile for KMC simulation, vibrational frequency analysis is used to obtain ZPE and the entropy ($\Delta S^{\neq}$) values for the system. For elementary reactions, the free energy barriers ($\Delta G^{\neq}$) are given by

$$\Delta G^{\neq} = \Delta E_{0K}^{\neq} + \Delta\left(E_{0K\to T}^{\neq}\right) + \Delta ZPE^{\neq} - T\Delta S^{\neq} \tag{15}$$

$$\Delta ZPE^{\neq} = \frac{1}{2}h\left(\sum v_{transitional\ state} + \sum v_{initial\ state}\right) \tag{16}$$

$$\Delta SE^{\neq} = k\ln\left(\frac{q_{transitional\ state}}{q_{initial\ state}}\right) \tag{17}$$

where q and ν are the partition function and vibration frequency, respectively.

Given the value of H_2/CO_2 ratio (y) and total pressure (P in atm), the equilibrium conversion to CH_3OH and CO could be obtained from the reactions thermodynamics equilibrium as expressed below:

$$e^{-\frac{\Delta G_{CH_3OH}^{\neq}\times 1.6\times 10^{-19}}{1.38\times 10^{-23}\times T}} = \frac{p_{CH_3OH}\left(p_{CH_3OH}+p_{CO}\right)}{\left(\frac{P}{1+y}-p_{CH_3OH}-p_{CO}\right)\left(\frac{yP}{1+y}-yp_{CH_3OH}-p_{CO}\right)^{y}} \tag{18}$$

$$e^{-\frac{\Delta G_{CO}^{\neq}\times 1.6\times 10^{-19}}{1.38\times 10^{-23}\times T}} = \frac{p_{CO}\left(p_{CH_3OH}+p_{CO}\right)}{\left(\frac{P}{1+y}-p_{CH_3OH}-p_{CO}\right)\left(\frac{yP}{1+y}-yp_{CH_3OH}-p_{CO}\right)} \tag{19}$$

where $\Delta G_{CH_3OH}^{\neq}$ and $\Delta G_{CO}^{\neq}$ are the free energy changes (in eV) for CH_3OH and CO, and p_{CH_3OH} and p_{CO} are the partial pressure (in atm) of CH_3OH and CO. The value of p_{CH_3OH} and p_{CO} are obtained by solving Eqs. (18) and (19) simultaneously. Thus, the conversion to CH_3OH and CO is given by Eqs. (20) and (21), respectively:

$$C_{CH_3OH} = \frac{p_{CH_3OH}}{p_{CO_2 init}} = \frac{p_{CH_3OH}}{P/(1+y)} \tag{20}$$

$$C_{CO} = \frac{p_{CO}}{p_{CO_2 init}} = \frac{p_{CO}}{P/(1+y)} \tag{21}$$

6.2. Reactor

The CH_3OH plant setup consists of various unit operation equipment, such as mixers, heaters, coolers, heat exchangers, separator, distillation column, and reactor. The reactors used for this process are fixed bed and fluidized bed reactor (Kim et al., 2001; Natesakhawat et al., 2013). Fig. 10 presents fluidized bed batch reactor setup.

Fluidized bed reactor is a two-phase heterogeneous scheme in which the catalysts are suspended in a fluid-like manner to provide a well dispersed catalyst bed (K. Li et al., 2014). To prevent sedimentation of catalyst, a magnetic stirrer is incorporated for agitation. The hydrogenation reaction begins by feeding H_2 and CO_2 into the airtight reactor. The sample is obtained by a gas tight syringe or an on-line automatic sampling system in a fixed time interval.

The actual design in different research groups slightly varies, for example, some incorporated a cooler to remove the heat, whereas others employed water-bath to stabilize the temperature of the reactor. An efficient and suitable reactor design is yet to be achieved because limited reports are available. Therefore, developing the course of reactor design is a promising technique that could optimize the efficiency of CO_2 conversion to biorenewable fuel. On the other hand, a fluidized bed reactor can provide a simple system to examine the performance of various catalysts in practice.

6.3. Process intensification

As discussed in section 4, several factors influence the performance of a CO_2 catalytic conversion system. A combination of the

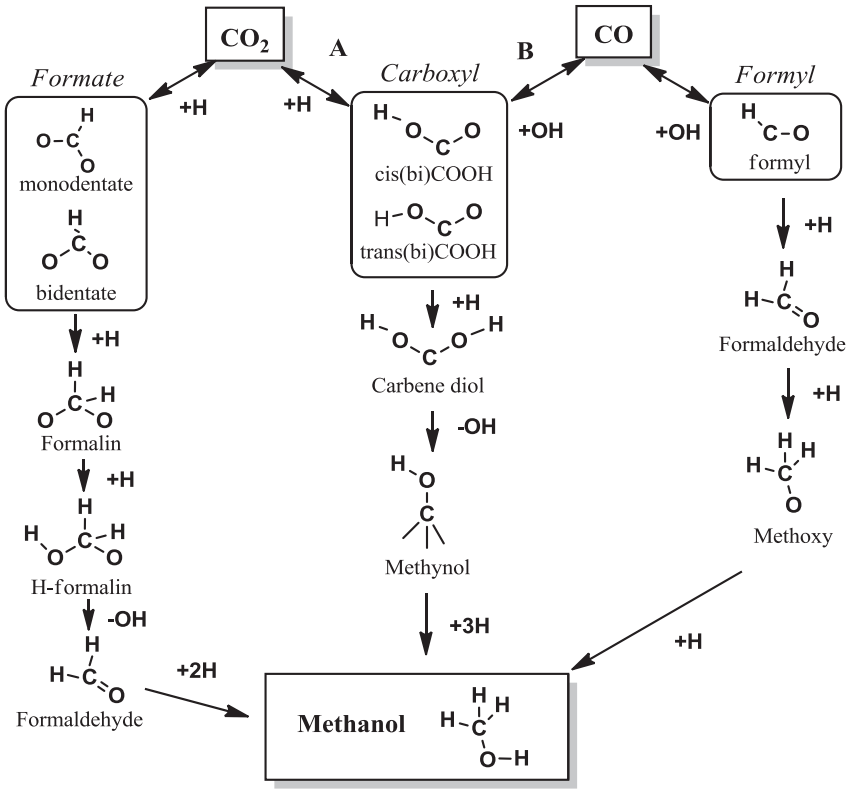

Fig. 11. Mechanistic pathways for conversion of CO and CO_2 to methanol over Cu. The water–gas shift mechanism through a carboxyl intermediate is seen across the top (Yang et al., 2013).

optimum values of factors, such as GHSV and operating pressure, could intensify the process (Gaikwad et al., 2016). Furthermore, the combination of enhanced catalyst design with improved reactor design, as well as microreactors that intensifies the process and enables faster transient, exhibit potential. Recycling of the stream that consists of unconverted CO_2 and H_2 and production of CO via RWGS reaction are also promising.

Yang et al. (2013) investigated CH_3OH synthesis from a mixture of CO_2, CO, H_2, and small amount of H_2O over Cu-based catalyst at low temperature and pressure (403–453 K, 0.6 MPa). They reported that a small amount of H_2O assisted CH_3OH formation, specifically from CO than from CO_2. Higher temperature favors CO_2 conversion, whereas lower temperature favors CO conversion. They proposed a new mechanism for CH_3OH synthesis via hydrogenating a mixture of CO_2 and CO based on DFT. This mechanism shows the interconversion of CO and CO_2 via a carboxyl (H–O–C–O) intermediate in which the O–CO bond is activated. The carboxyl intermediate is generated from CO_2 (through route A) and from CO (through route B), as illustrated in Fig. 11. The proposed mechanism for CH_3OH production through the carboxyl intermediate is shown at the center column.

7. Conclusion

The robust utilization of CO_2 is important for global environmental hazard mitigation. In this work, the recent development in catalytic hydrogenation of CO_2 to CH_3OH and other specialty chemicals is presented. Recently, much effort is directed toward substituting CO_2 for CO in CH_3OH synthesis. The major issue is the choice of catalyst for efficient performance. The performance of $CuO/ZnO/Al_2O_3$, being the conventional catalyst for CH_3OH synthesis, is plagued with unwanted CO formation via the RWGS resulting to a very low CH_3OH selectivity. The poor performance of the conventional catalyst is also linked with the fact that CO_2 is kinetically and thermodynamically stable.

To solve this issue, the reaction mechanism for the CO_2 hydrogenation is investigated. Generally, catalytic reduction of CO_2 has two reaction routes: first, the desired mechanism via a formate intermediate; and second, a RWGS via CO_2 decomposition to CO. Consequently, a rational design of a catalyst that will minimize selectivity to CO is needed. Several formulations of supported metal oxide, such as transition metals, transition metal carbide, and noble metals, are investigated. However, the performances of these formulations are not satisfactory. The activity should be improved by using a suitable support or promoter. Therefore, the effect of promoters is studied. Promoters with mild basicity and amphoteric oxides help to reduce formation of CO, whereas promoters with higher basicity stimulates the selectivity to CO. Solid acid supports promote DME formation by cracking CH_3OH. Furthermore, combining the optimum values of the operating factors such as GHSV and operating pressure, as well as recycling the stream that consist of unconverted CO_2 and H_2, and CO (produced via RWGS reaction to the reactor), is promising for intensifying the process.

Acknowledgement

We gratefully acknowledge the High Impact Research (HIR) grant from the University of Malaya for fully funding this study through Project No. “D000011-16001.” We also appreciate the

support of Chemical Engineering Department with RP015-2012D grant.

References

Abnisa, F., Daud, W.M.A.W., 2015. Optimization of fuel recovery through the stepwise co-pyrolysis of palm shell and scrap tire. Energy Convers. Manag. 99, 334–345.

Alaba, P.A., Sani, Y.M., Daud, W.M.A.W., 2015a. Kaolinite properties and advances for solid acid and basic catalyst synthesis. RSC Adv. 5 (122), 101127–101147.

Alaba, P.A., Sani, Y.M., Daud, W.M.A.W., 2015b. Synthesis and characterization of hierarchical nanoporous HY zeolites from acid-activated kaolin. Chin. J. Catal. 36 (11), 1846–1851.

Alaba, P.A., Sani, Y.M., DAUD, W.M.A.W., 2016a. Efficient biodiesel production via solid superacid catalysis: a critical review on recent breakthrough. RSC Adv. 6 (82), 78351–78368.

Alaba, P.A., Sani, Y.M., Mohammed, I.Y., Abakr, Y.A., Daud, W.M.A.W., 2016b. Synthesis and application of hierarchical mesoporous HZSM-5 for biodiesel production from shea butter. J. Taiwan Inst. Chem. Eng. 59, 405–412.

Alaba, P.A., Sani, Y.M., Mohammed, I.Y., Daud, W., Ashri, W.M., 2016c. Insight into catalyst deactivation mechanism and suppression techniques in thermocatalytic deoxygenation of bio-oil over zeolites. Rev. Chem. Eng. 32 (1), 71–91.

Alaba, P.A., Sani, Y.M., Daud, W.M.A.W., 2016d. A comparative study on thermal decomposition behavior of biodiesel samples produced from shea butter over micro-and mesoporous ZSM-5 zeolites using different kinetic models. J. Therm. Anal. Calorim. 1–6.

An, X., Li, J., Zuo, Y., Zhang, Q., Wang, D., Wang, J., 2007. A Cu/Zn/Al/Zr fibrous catalyst that is an improved CO2 hydrogenation to methanol catalyst. Catal. Lett. 118 (3–4), 264–269.

Arena, F., Barbera, K., Italiano, G., Bonura, G., Spadaro, L., Frusteri, F., 2007. Synthesis, characterization and activity pattern of Cu–ZnO/ZrO_2 catalysts in the hydrogenation of carbon dioxide to methanol. J. Catal. 249 (2), 185–194.

Back, S., Yeom, M.S., Jung, Y., 2015. Active sites of Au and Ag nanoparticle catalysts for CO_2 electroreduction to CO. ACS Catal. 5 (9), 5089–5096.

Bahruji, H., Bowker, M., Hutchings, G., Dimitratos, N., Wells, P., Gibson, E., …, Lalev, G., 2016. Pd/ZnO catalysts for direct CO_2 hydrogenation to methanol. J. Catal. http://dx.doi.org/10.1016/j.jcat.2016.03.017.

Bai, S., Jiang, J., Zhang, Q., Xiong, Y., 2015. Steering charge kinetics in photocatalysis: intersection of materials syntheses, characterization techniques and theoretical simulations. Chem. Soc. Rev. 44 (10), 2893–2939.

Bansode, A., Urakawa, A., 2014. Towards full one-pass conversion of carbon dioxide to methanol and methanol-derived products. J. Catal. 309, 66–70.

Bauer, N., Mouratiadou, I., Luderer, G., Baumstark, L., Brecha, R.J., Edenhofer, O., Kriegler, E., 2013. Global fossil energy markets and climate change mitigation–an analysis with REMIND. Clim. change 1–14.

Behrens, M., Zander, S., Kurr, P., Jacobsen, N., Senker, J.R., Koch, G., …, Schlögl, R., 2013. Performance improvement of nanocatalysts by promoter-induced defects in the support material: methanol synthesis over Cu/ZnO: Al. J. Am. Chem. Soc. 135 (16), 6061–6068.

Berardi, S., Drouet, S., Francàs, L., Gimbert-Suriñach, C., Guttentag, M., Richmond, C., …, Llobet, A., 2014. Molecular artificial photosynthesis. Chem. Soc. Rev. 43 (22), 7501–7519.

Bonura, G., Cordaro, M., Spadaro, L., Cannilla, C., Arena, F., Frusteri, F., 2013. Hybrid Cu–ZnO–ZrO_2/H-ZSM5 system for the direct synthesis of DME by CO_2 hydrogenation. Appl. Catal. B Environ. 140, 16–24.

Borodko, Y., Somorjai, G., 1999. Catalytic hydrogenation of carbon oxides–a 10-year perspective. Appl. Catal. A General 186 (1), 355–362.

Budzianowski, W.M., 2012. Value-added carbon management technologies for low CO_2 intensive carbon-based energy vectors. Energy 41 (1), 280–297.

Change, C., 2007. Synthesis Report. Contribution of Working Groups I, II and III to the Fourth Assessment Report of the Intergovernmental Panel on Climate Change. IPCC, Geneva, Switzerland.

Chen, Y., Choi, S., Thompson, L.T., 2015. Low-temperature CO_2 hydrogenation to liquid products via a heterogeneous cascade catalytic system. ACS Catal. 5 (3), 1717–1725.

Chen, Y., Choi, S., Thompson, L.T., 2016. Low temperature CO_2 hydrogenation to alcohols and hydrocarbons over Mo_2 C supported metal catalysts. J. Catal. http://dx.doi.org/10.1016/j.jcat.2016.01.016.

Collins, S.E., Baltanás, M.A., Fierro, J.L.G., Bonivardi, A.L., 2002. Gallium–hydrogen bond formation on gallium and gallium–palladium silica-supported catalysts. J. Catal. 211 (1), 252–264.

Costentin, C., Robert, M., Savéant, J.-M., 2013. Catalysis of the electrochemical reduction of carbon dioxide. Chem. Soc. Rev. 42 (6), 2423–2436.

Cuéllar-Franca, R.M., Azapagic, A., 2015. Carbon capture, storage and utilisation technologies: a critical analysis and comparison of their life cycle environmental impacts. J. CO_2 Util. 9, 82–102.

Dubois, J.-L., Sayama, K., Arakawa, H., 1992. CO_2 hydrogenation over carbide catalysts. Chem. Lett. (1), 5–8.

Evans, J., Liu, D.-j., Tammaro, M., 2002. From atomistic lattice-gas models for surface reactions to hydrodynamic reaction-diffusion equations. Chaos An Interdiscip. J. Nonlinear Sci. 12 (1), 131–143.

Fisher, I.A., Bell, A.T., 1997. In-situinfrared study of methanol synthesis from H_2/CO_2 over Cu/SiO_2 and Cu/ZrO_2/SiO_2. J. Catal. 172 (1), 222–237.

Fisher, I.A., Bell, A.T., 1999. A mechanistic study of methanol decomposition over Cu/SiO_2, ZrO_2/SiO_2, and Cu/ZrO_2/SiO_2. J. Catal. 184 (2), 357–376.

Frusteri, F., Cordaro, M., Cannilla, C., Bonura, G., 2015. Multifunctionality of Cu–ZnO–ZrO_2/H-ZSM5 catalysts for the one-step CO_2-to-DME hydrogenation reaction. Appl. Catal. B Environ. 162, 57–65.

Fujitani, T., Saito, M., Kanai, Y., Watanabe, T., Nakamura, J., Uchijima, T., 1995. Development of an active Ga_2O_3 supported palladium catalyst for the synthesis of methanol from carbon dioxide and hydrogen. Appl. Catal. A General 125 (2), L199–L202.

Gaikwad, R., Bansode, A., Urakawa, A., 2016. High-pressure advantages in stoichiometric hydrogenation of carbon dioxide to methanol. J. Catal. http://dx.doi.org/10.1016/j.jcat.2016.02.005.

Gi-Won, Jeon, Wonje, Sin, Kyu-Wan, Lee, 1999. Concurrent production of methanol and dimethyl ether from carbon dioxide hydrogenation: investigation of reaction conditions. Bull. Korean Chem. Soc. 20 (9), 993–998.

Gotti, A., Prins, R., 1998. Basic metal oxides as co-catalysts in the conversion of synthesis gas to methanol on supported palladium catalysts. J. Catal. 175 (2), 302–311.

Graaf, G., Sijtsema, P., Stamhuis, E., Joosten, G., 1986. Chemical equilibria in methanol synthesis. Chem. Eng. Sci. 41 (11), 2883–2890.

Graaf, G., Stamhuis, E., Beenackers, A., 1988. Kinetics of low-pressure methanol synthesis. Chem. Eng. Sci. 43 (12), 3185–3195.

Hong, Q.-J., Liu, Z.-P., 2010. Mechanism of CO_2 hydrogenation over Cu/ZrO_2 (212) interface from first-principles kinetics Monte Carlo simulations. Surf. Sci. 604 (21), 1869–1876.

Hong, Z.-s., Cao, Y., Deng, J.-f., Fan, K.-n., 2002. CO_2 hydrogenation to methanol over Cu/ZnO/Al_2O_3 catalysts prepared by a novel gel-network-coprecipitation method. Catal. Lett. 82 (1–2), 37–44.

Hu, B., Guild, C., Suib, S.L., 2013. Thermal, electrochemical, and photochemical conversion of CO_2 to fuels and value-added products. J. CO_2 Util. 1, 18–27.

Huo, Z., Hu, M., Zeng, X., Yun, J., Jin, F., 2012. Catalytic reduction of carbon dioxide into methanol over copper under hydrothermal conditions. Catal. today 194 (1), 25–29.

Hurst, T.F., Cockerill, T.T., Florin, N.H., 2012. Life cycle greenhouse gas assessment of a coal-fired power station with calcium looping CO_2 capture and offshore geological storage. Energy & Environ. Sci. 5 (5), 7132–7150.

Inui, T., Takeguchi, T., 1991. Effective conversion of carbon dioxide and hydrogen to hydrocarbons. Catal. today 10 (1), 95–106.

Jeong, H., Cho, C.H., Kim, T.H., 2012. Effect of Zr and pH in the preparation of Cu/ZnO catalysts for the methanol synthesis by CO_2 hydrogenation. React. Kinet. Mech. Catal. 106 (2), 435–443.

Jiang, X., Koizumi, N., Guo, X., Song, C., 2015. Bimetallic Pd–Cu catalysts for selective CO_2 hydrogenation to methanol. Appl. Catal. B Environ. 170, 173–185.

Jongerius, A.L., Gosselink, R.W., Dijkstra, J., Bitter, J.H., Bruijnincx, P.C., Weckhuysen, B.M., 2013. Carbon nanofiber supported transition-metal carbide catalysts for the hydrodeoxygenation of guaiacol. Chem. Cat. Chem. 5 (10), 2964–2972.

Jun, K.-W., Rama Rao, K., Jung, M.-H., Lee, K.-W., 1998. The CO~2 hydrogenation toward the mixture of methanol and dimethyl ether: investigation of hybrid catalysts. Bull. Korean Chem. Soc. 19, 466–470.

Khatib, H., 2012. IEA world energy outlook 2011—A comment. Energy policy 48, 737–743.

Kim, J.S., Kim, H.K., Lee, S.B., Choi, M.J., Lee, K.W., Kang, Y., 2001. Characteristics of carbon dioxide hydrogenation in a fluidized bed reactor. Korean J. Chem. Eng. 18 (4), 463–467.

Koizumi, N., Jiang, X., Kugai, J., Song, C., 2012. Effects of mesoporous silica supports and alkaline promoters on activity of Pd catalysts in CO_2 hydrogenation for methanol synthesis. Catal. today 194 (1), 16–24.

Kunkes, E.L., Studt, F., Abild-Pedersen, F., Schlögl, R., Behrens, M., 2015. Hydrogenation of CO_2 to methanol and CO on Cu/ZnO/Al_2O_3: is there a common intermediate or not? J. Catal. 328, 43–48.

Lachowska, M., Skrzypek, J., 2004. Methanol synthesis from carbon dioxide and hydrogen over Mn-promoted copper/zinc/zirconia catalysts. React. Kinet. Catal. Lett. 83 (2), 269–273.

Le Valant, A., Comminges, C., Tisseraud, C., Canaff, C., Pinard, L., Pouilloux, Y., 2015. The Cu–ZnO synergy in methanol synthesis from CO_2, Part 1: origin of active site explained by experimental studies and a sphere contact quantification model on Cu+ ZnO mechanical mixtures. J. Catal. 324, 41–49.

Lee, J.S., Han, S.H., Kim, H.G., Lee, K.H., Kim, Y.G., 2000. Effects of space velocity on methanol synthesis from CO_2/CO/H_2 over Cu/ZnO/Al_2O_3 catalyst. Korean J. Chem. Eng. 17 (3), 332–336.

Li, K., An, X., Park, K.H., Khraisheh, M., Tang, J., 2014. A critical review of CO_2 photoconversion: catalysts and reactors. Catal. today 224, 3–12.

Li, L., Mao, D., Yu, J., Guo, X., 2015. Highly selective hydrogenation of CO_2 to methanol over CuO–ZnO–ZrO_2 catalysts prepared by a surfactant-assisted co-precipitation method. J. Power Sources 279, 394–404.

Li, M.M.-J., Zeng, Z., Liao, F., Hong, X., Tsang, S.C.E., 2016. Enhanced CO_2 hydrogenation to methanol over CuZn nanoalloy in Ga modified Cu/ZnO catalysts. J. Catal. http://dx.doi.org/10.1016/j.jcat.2016.03.020.

Liang, X.-L., Dong, X., Lin, G.-D., Zhang, H.-B., 2009. Carbon nanotube-supported

Pd–ZnO catalyst for hydrogenation of CO_2 to methanol. Appl. Catal. B Environ. 88 (3), 315–322.
Liang, X.-L., Xie, J.-R., Liu, Z.-M., 2015. A novel Pd-decorated carbon nanotubes-promoted Pd-ZnO catalyst for CO_2 hydrogenation to methanol. Catal. Lett. 145 (5), 1138–1147.
Liaw, B., Chen, Y., 2001. Liquid-phase synthesis of methanol from CO_2/H_2 over ultrafine CuB catalysts. Appl. Catal. A General 206 (2), 245–256.
Liu, X.-M., Lu, G., Yan, Z.-F., 2005. Nanocrystalline zirconia as catalyst support in methanol synthesis. Appl. Catal. A General 279 (1), 241–245.
Ma, S., Kenis, P.J., 2013. Electrochemical conversion of CO_2 to useful chemicals: current status, remaining challenges, and future opportunities. Curr. Opin. Chem. Eng. 2 (2), 191–199.
Ma, J., Sun, N., Zhang, X., Zhao, N., Xiao, F., Wei, W., Sun, Y., 2009. A short review of catalysis for CO_2 conversion. Catal. today 148 (3), 221–231.
McCollum, D., Bauer, N., Calvin, K., Kitous, A., Riahi, K., 2014. Fossil resource and energy security dynamics in conventional and carbon-constrained worlds. Clim. change 123 (3–4), 413–426.
McGlade, C., Ekins, P., 2015. The geographical distribution of fossil fuels unused when limiting global warming to 2 °C. Nature 517 (7533), 187–190.
Mendes, L., de Medeiros, J.L., Alves, R.M., Araújo, O.Q., 2014. Production of methanol and organic carbonates for chemical sequestration of CO_2 from an NGCC power plant. Clean Technol. Environ. Policy 16 (6), 1095–1105.
Mikkelsen, M., Jørgensen, M., Krebs, F.C., 2010. The teraton challenge. A review of fixation and transformation of carbon dioxide. Energy & Environ. Sci. 3 (1), 43–81.
Mohammed, I.Y., Kazi, F.K., Yusup, S., Alaba, P.A., Sani, Y.M., Abakr, Y.A., 2016. Catalytic intermediate pyrolysis of napier grass in a fixed bed reactor with ZSM-5, HZSM-5 and zinc-exchanged zeolite-A as the catalyst. Energies 9 (4), 246.
Natesakhawat, S., Ohodnicki Jr., P.R., Howard, B.H., Lekse, J.W., Baltrus, J.P., Matranga, C., 2013. Adsorption and deactivation characteristics of Cu/ZnO-based catalysts for methanol synthesis from carbon dioxide. Top. Catal. 56 (18–20), 1752–1763.
Neurock, M., Wasileski, S.A., Mei, D., 2004. From first principles to catalytic performance: tracking molecular transformations. Chem. Eng. Sci. 59 (22), 4703–4714.
Nomura, N., Tagawa, T., Goto, S., 1998. Effect of acid-base properties on copper catalysts for hydrogenation of carbon dioxide. React. Kinet. Catal. Lett. 63 (1), 21–25.
Olah, G.A., 2004. After oil and gas: methanol economy. Catal. Lett. 93 (1), 1–2.
Olah, G.A., Molnar, A., 2003. Hydrocarbon Chemistry. John Wiley & Sons.
Oyola-Rivera, O., Baltanás, M.A., Cardona-Martínez, N., 2015. CO_2 hydrogenation to methanol and dimethyl ether by Pd–Pd 2 Ga catalysts supported over Ga_2O_3 polymorphs. J. CO_2 Util. 9, 8–15.
Porosoff, M.D., Yang, X., Boscoboinik, J.A., Chen, J.G., 2014. Molybdenum carbide as alternative catalysts to precious metals for highly selective reduction of CO_2 to CO. Angew. Chem. Int. Ed. 53 (26), 6705–6709.
Prieto, G., Zečević, J., Friedrich, H., de Jong, K.P., de Jongh, P.E., 2013. Towards stable catalysts by controlling collective properties of supported metal nanoparticles. Nat. Mater. 12 (1), 34–39.
Qi, G.-X., Fei, J.-H., Hou, Z.-Y., Zheng, X.-M., 2001a. Methanol synthesis by co_2 hydrogenation over titanium modified γ-al_2o_3 supported copper catalysts. React. Kinet. Catal. Lett. 73 (1), 151–160.
Qi, G.-X., Zheng, X.-M., Fei, J.-H., Hou, Z.-Y., 2001b. Low-temperature methanol synthesis catalyzed over Cu/γ-Al_2O_3–TiO_2 for CO_2 hydrogenation. Catal. Lett. 72 (3–4), 191–196.
Qu, Y., Duan, X., 2013. Progress, challenge and perspective of heterogeneous photocatalysts. Chem. Soc. Rev. 42 (7), 2568–2580.
Ravanchi, M.T., Sahebdelfar, S., 2014. Carbon dioxide capture and utilization in petrochemical industry: potentials and challenges. Appl. Petrochem. Res. 4 (1), 63–77.
Reuter, K., Frenkel, D., Scheffler, M., 2004. The steady state of heterogeneous catalysis, studied by first-principles statistical mechanics. Phys. Rev. Lett. 93 (11), 116105.
Roy, S.C., Varghese, O.K., Paulose, M., Grimes, C.A., 2010. Toward solar fuels: photocatalytic conversion of carbon dioxide to hydrocarbons. Acs Nano 4 (3), 1259–1278.
Saito, M., Murata, K., 2004. Development of high performance Cu/ZnO-based catalysts for methanol synthesis and the water-gas shift reaction. Catal. Surv. Asia 8 (4), 285–294.
Sakakura, T., Choi, J.-C., Yasuda, H., 2007. Transformation of carbon dioxide. Chem. Rev. 107 (6), 2365–2387.
Sani, Y.M., Alaba, P.A., Raji-Yahya, A.O., Aziz, A.A., Daud, W.M.A.W., 2016a. Acidity and catalytic performance of Yb-doped/Zr in comparison with/Zr catalysts synthesized via different preparatory conditions for biodiesel production. J. Taiwan Inst. Chem. Eng. 59, 195–204.
Sani, Y.M., Alaba, P.A., Raji-Yahya, A.O., Aziz, A.A., Daud, W.M.A.W., 2016b. Facile synthesis of sulfated mesoporous Zr/ZSM-5 with improved Brønsted acidity and superior activity over SZr/Ag, SZr/Ti, and SZr/W in transforming UFO into biodiesel. J. Taiwan Inst. Chem. Eng. 60, 247–257.
Sanna, A., Uibu, M., Caramanna, G., Kuusik, R., Maroto-Valer, M., 2014. A review of mineral carbonation technologies to sequester CO_2. Chem. Soc. Rev. 43 (23), 8049–8080.
Schweitzer, N.M., Schaidle, J.A., Ezekoye, O.K., Pan, X., Linic, S., Thompson, L.T., 2011. High activity carbide supported catalysts for water gas shift. J. Am. Chem. Soc. 133 (8), 2378–2381.
Sendner, C., Sakong, S., Groß, A., 2006. Kinetic Monte Carlo simulations of the partial oxidation of methanol on oxygen-covered Cu (110). Surf. Sci. 600 (16), 3258–3265.
Setthapun, W., Bej, S.K., Thompson, L.T., 2008. Carbide and nitride supported methanol steam reforming catalysts: parallel synthesis and high throughput screening. Top. Catal. 49 (1–2), 73–80.
Shen, W.-J., Jun, K.-W., Choi, H.-S., Lee, K.-W., 2000. Thermodynamic investigation of methanol and dimethyl ether synthesis from CO_2 hydrogenation. Korean J. Chem. Eng. 17 (2), 210–216.
Shen, W.-J., Okumura, M., Matsumura, Y., Haruta, M., 2001. The influence of the support on the activity and selectivity of Pd in CO hydrogenation. Appl. Catal. A General 213 (2), 225–232.
Shido, T., Iwasawa, Y., 1993. The effect of coadsorbates in reverse water-gas shift reaction on ZnO, in relation to reactant-promoted reaction mechanism. J. Catal. 140 (2), 575–584.
Song, Y., Liu, X., Xiao, L., Wu, W., Zhang, J., Song, X., 2015. Pd-Promoter/MCM-41: a highly effective bifunctional catalyst for conversion of carbon dioxide. Catal. Lett. 145 (6), 1272–1280.
Szailer, T., Novák, É., Oszkó, A., Erdőhelyi, A., 2007. Effect of H_2S on the hydrogenation of carbon dioxide over supported Rh catalysts. Top. Catal. 46 (1–2), 79–86.
Tabatabaei, J., Sakakini, B., Waugh, K., 2006. On the mechanism of methanol synthesis and the water-gas shift reaction on ZnO. Catal. Lett. 110 (1–2), 77–84.
Tang, Q.-L., Hong, Q.-J., Liu, Z.-P., 2009. CO_2 fixation into methanol at Cu/ZrO_2 interface from first principles kinetic Monte Carlo. J. Catal. 263 (1), 114–122.
Temel, B., Meskine, H., Reuter, K., Scheffler, M., Metiu, H., 2007. Does phenomenological kinetics provide an adequate description of heterogeneous catalytic reactions? J. Chem. Phys. 126 (20), 204711.
Tidona, B., Urakawa, A., von Rohr, P.R., 2013. High pressure plant for heterogeneous catalytic CO_2 hydrogenation reactions in a continuous flow microreactor. Chem. Eng. Process. Process Intensif. 65, 53–57.
Tisseraud, C., Comminges, C., Belin, T., Ahouari, H., Soualah, A., Pouilloux, Y., Le Valant, A., 2015. The Cu–ZnO synergy in methanol synthesis from CO_2, Part 2: origin of the methanol and CO selectivities explained by experimental studies and a sphere contact quantification model in randomly packed binary mixtures on Cu–ZnO coprecipitate catalysts. J. Catal. 330, 533–544.
Tominaga, H., Nagai, M., 2005. Density functional study of carbon dioxide hydrogenation on molybdenum carbide and metal. Appl. Catal. A General 282 (1), 5–13.
Toyir, J., de la Piscina, P.R.R., Fierro, J.L.G., Homs, N. s., 2001. Highly effective conversion of CO_2 to methanol over supported and promoted copper-based catalysts: influence of support and promoter. Appl. Catal. B Environ. 29 (3), 207–215.
Tuomi, S., Guil-Lopez, R., Kallio, T., 2016. Molybdenum carbide nanoparticles as a catalyst for the hydrogen evolution reaction and the effect of pH. J. Catal. 334, 102–109.
Valipour, M., 2012a. Comparison of surface irrigation simulation models: full hydrodynamic, zero inertia, kinematic wave. J. Agric. Sci. 4 (12), 68.
Valipour, M., 2012b. Sprinkle and trickle irrigation system design using tapered pipes for pressure loss adjusting. J. Agric. Sci. 4 (12), 125.
Wang, J.B., Lee, H.-K., Huang, T.-J., 2002. Synergistic catalysis of carbon dioxide hydrogenation into methanol by yttria-doped ceria/γ-alumina-supported copper oxide catalysts: effect of support and dopant. Catal. Lett. 83 (1–2), 79–86.
Windle, C.D., Perutz, R.N., 2012. Advances in molecular photocatalytic and electrocatalytic CO_2 reduction. Coord. Chem. Rev. 256 (21), 2562–2570.
Xu, A., Indala, S., Hertwig, T.A., Pike, R.W., Knopf, F.C., Yaws, C.L., Hopper, J.R., 2005. Development and integration of new processes consuming carbon dioxide in multi-plant chemical production complexes. Clean Technol. Environ. Policy 7 (2), 97–115.
Xu, W., Ramirez, P.J., Stacchiola, D., Rodriguez, J.A., 2014. Synthesis of α-MoC1-x and β-MoCy catalysts for CO2 hydrogenation by thermal carburization of Mo-oxide in hydrocarbon and hydrogen mixtures. Catal. Lett. 144 (8), 1418–1424.
Xu, J., Su, X., Liu, X., Pan, X., Pei, G., Huang, Y., …, Geng, H., 2016. Methanol Synthesis from CO_2 and H_2 over Pd/ZnO/Al_2O_3: catalyst structure dependence of methanol selectivity. Appl. Catal. A General 514, 51–59.
Yang, C., Ma, Z., Zhao, N., Wei, W., Hu, T., Sun, Y., 2006. Methanol synthesis from CO_2-rich syngas over a ZrO_2 doped CuZnO catalyst. Catal. today 115 (1), 222–227.
Yang, Y., Mims, C.A., Mei, D., Peden, C.H., Campbell, C.T., 2013. Mechanistic studies of methanol synthesis over Cu from $CO/CO_2/H_2/H_2O$ mixtures: the source of C in methanol and the role of water. J. Catal. 298, 10–17.
Yannopoulos, S.I., Lyberatos, G., Theodossiou, N., Li, W., Valipour, M., Tamburrino, A., Angelakis, A.N., 2015. Evolution of water lifting devices (pumps) over the centuries worldwide. Water 7 (9), 5031–5060.
Yin, S., Ge, Q., 2012. Selective CO_2 hydrogenation on the γ-Al_2O_3 supported bimetallic Co–Cu catalyst. Catal. today 194 (1), 30–37.
Yui, T., Tamaki, Y., Sekizawa, K., Ishitani, O., 2011. Photocatalytic reduction of CO_2: from molecules to semiconductors. Photocatalysis 151–184.
Zangeneh, F.T., Sahebdelfar, S., Ravanchi, M.T., 2011. Conversion of carbon dioxide to valuable petrochemicals: an approach to clean development mechanism. J. Nat. Gas Chem. 20 (3), 219–231.

Zhdanov, V.P., 2002. Impact of surface science on the understanding of kinetics of heterogeneous catalytic reactions. Surf. Sci. 500 (1), 966–985.

Peter Adeniyi Alaba was born and raised in Kwara State, Nigeria. He did his undergraduate study in Chemical Engineering at the Federal University of Technology Minna. He received his MEngSc by research in Chemical Engineering from the University of Malaya under the supervision of Prof. Wan Mohd Ashri Wan Daud. He was appointed as a research assistant at the University of Malaya in 2013 till date. His research interests lie in rational design of tailored solid acid catalysts for efficient green energy production, computational chemistry and environmental engineering. He has published more than 11 papers in reputed journals and has been serving as a reviewer for reputable journals since 2015.